JOURNAL OF ADVANCED MECHANICAL ENGINEERING APPLICATIONS
VOL. 1 NO. 1 (2020) 36-45

JAMEA

Journal homepage: http://penerbit.uthm.edu.my/jamea

e-ISSN : XXXX-XXXX

Journal of Advanced Mechanical Engineering Applications

Effect of combined Ce and Er Addition on Solidification, Microstructure of the Al-7Si-alloy

Faraj Saeid Adrees Majeed[1*], Mohd Azlan Suhaimi[1], Nordin Bin Mohd Yusof[1], Rosli Bin Ahmad[2], Mohammed Basher Asmael[2], Mohd Sallehuddin Hj.Yusof[2]

[1]Department of Manufacturing Engineering, School of Mechanical Engineering, University Technology Malaysia, 81310 Skudai, Johor, MALAYSIA

[2]Department of Manufacturing Engineering, Faculty of Mechanical Engineering, Universiti Tun Hussein Onn Malaysia, 86400 Parit Raja, Batu Pahat, Johor, MALAYSIA

*Corresponding Author

DOI: https://doi.org/10.30880/jamea.2020.01.01.005
Received 20 September 2019; Accepted 07 January 2020; Available online 31 January 2020

Abstract: This paper highlights the effects of the additions of two rare earth elements (REEs) (Ce and Er) on microstructure and to investigate the characteristic temperatures during solidification of the modified alloy. Five changes of Al-7Si alloys with xEr+xCe additions (x=0.15, 0.25, 0.4, 0.5 and 0.75) were produced by casting technique via the solidification parameters examined using computer-aided cooling curve thermal analysis (CA-CCTA). The thermal analysis tests were carried out for each one by using a thermal analysis system that includes (K-type Thermocouple, EPAD-TH8-K, EPAD-Baes2 and Laptop with Dewesoft-7.5-Lt). To estimate the change in microstructure and solidification as a result of adding (Ce+Er) additions, the obtained result showed that the growth $T_G^{\text{Al-Phase}}$ and nucleation $T_N^{\text{Al-Phase}}$ temperatures decreased to lower temperatures 614.7°C and 615.5°C respectively as the amount Ce, Er increased.

Keywords: Microstructure, Thermal Analysis, Er: Erbium, Ce: Cerium

1. Introduction

Cast Aluminum-silicon (AI-Si) alloys are widely used in the automotive, aerospace and general engineering industries because of their excellent properties such as good castability, low coefficient of thermal expansion, high strength-to-weight ratio and superior corrosion resistance. Aluminium alloys are used extensively because of their high strength to weight ratio, good machinability, corrosion resistance, optimum surface finish, and high electrical and thermal conductivity [1].

Al-7Si alloy is mainly also used where excellent mechanical properties are required in castings of shape or dimensions requiring an alloy of excellent castability, in order to achieve the desired standard of soundness. The alloy is also used where resistance to corrosion is an important consideration, particularly where high strength is also required. Consequently, Al-7Si has its application in foods, chemicals, marines, electrical and many other industries and above all in road transport vehicles where it is used for cylinder blocks. The availability increases its potential uses in four conditions of heat treatment in both sand and chill castings. It is, in practice, a general-purpose high strength casting alloy [8].

*Corresponding author: safaraj@graduate.utm.my

There are several reasons for aluminium continued expansion into newer and broader fields of application. With the objectives of providing a lightweight and reasonably high mechanical property materials, saving cost and energy as well as reducing detrimental effects on the environment, aluminium industries are moving towards using secondary aluminium in the form of returns and scrap as a replacement for pure metals [12]. Furthermore, Al alloys are available in both cast and wrought forms, and about 20% of aluminium produced is used in the cast form mainly in the transportation sector [15]. Among commercial aluminium casting alloys, those with silicon as the primary alloying element are the most important ones mainly because of their excellent casting characteristics. The addition of Si to pure aluminium imparts high fluidity, unique feeding characteristics, low shrinkage and excellent hot cracking resistance. The high strength to weight ratio is one of their most exciting characteristics [17]. Engineering properties such as tensile strength and shear strength may be considerably different from those of the constituent materials [13].

The main contribution of this work is to investigate the influence of the interaction of Ce thoroughly, and Er concentrations on the quality of modification and refiner of Al-7Si alloy by monitoring the progress of specific metallurgical phase transformation parameters during solidification phases such as Al-Si phase. Besides, the work also investigates the effects of additions on the microstructure and the capability to react with major alloying elements such as Al, Si, and Mg forming compounds during solidification. These compounds play a significant role in the mechanical properties of these alloys. Besides that, the correlation between metallography examinations and mechanical properties with solidification characteristics is done to quantify in detail the effects of these elements on the quality of ternary Al-7Si alloy. The challenge within this research is to extend the limitations of Al-Si alloys.

1.1 Alloy Preparation and Addition of Elements

The Ce and Er addition levels are 0.1, 0.3, 0.5, 0.8 1 and 1.5 wt%. The added elements were first wrapped in aluminium foil and then plunged into the melt to ensure that they dissolved properly and evenly throughout the melt and stirred with a zirconia-coated steel rod for approximately 30 seconds for better dissolution. The melt temperature was maintained at 577 °C [3] and later increased to 750-760 °C for an adequate time to allow for complete melt homogenisation [6]. Additionally, 750±5 ºC was the applied pouring temperature. Before casting, the alloys were stirred and skimmed of its surface to remove any trash and other impurities. The molten alloy was then poured at the temperature of 730 ± 5 ˚C into the preheated moulds. Each material addition was allowed 10 min for homogenisation [9] before pouring. The melt was also stirred directly before sample pouring. Investment casting and the lost foam process involve an expendable mould as well as an expendable pattern [4].

1.2 Thermal Analysis

Thermal analysis was carried out by attaching a calibrated K-type thermocouple located in the middle of the preheated ceramic mould, which solidifies in slow conditions to determine the behaviour and detect the characteristic temperatures during alloy solidification. One thermocouple was used to provide additional information about solidification behaviour. This technique was developed by [2]. Backed who used it to register the beginning of nucleation and the coherency point of the dendrite structure [2]. To ensure radial heat flow during solidification, the mould was isolated at the top and bottom with Fiberfrax plates [11]. To facilitate the slow cooling rate to reveal more transformations during compression, all-ceramic moulds were preheated at 800 ºC for 30 minutes in a heating furnace (Carbolite). The thermal analysis results are experimentally obtained after the additions of Ce and Er to the base alloy and the effects are assessed according to the changes in the characteristic parameters from thermal analysis data and microstructure examination on the polished samples.

Table 1 - An example of a table

An example of a column heading	**Column A (*t*)**	**Column B (*t*)**
And an entry	1	2
And another entry	3	4
And another entry	5	6

1.3 Results

The cooling curves are plotted for the samples of base alloys (untreated alloys) and treated with (0.1, 0.3, 0.5, 0.8, 1.0 wt.%, and 1.5 wt.% Ce and Er according to the phase diagram of Ce, Er-Al [7] as shown in Figure 1. The primary cooling curve parameters of all the base alloys under different Ce and Er concentration as illustrated in Table 1. Figure 1shows the comparison between the cooling curves of the base alloy and treated with varying levels of Ce and Er. It can be seen that the addition of these elements has an impact on the cooling curves, especially in the hypoeutectic reaction region.

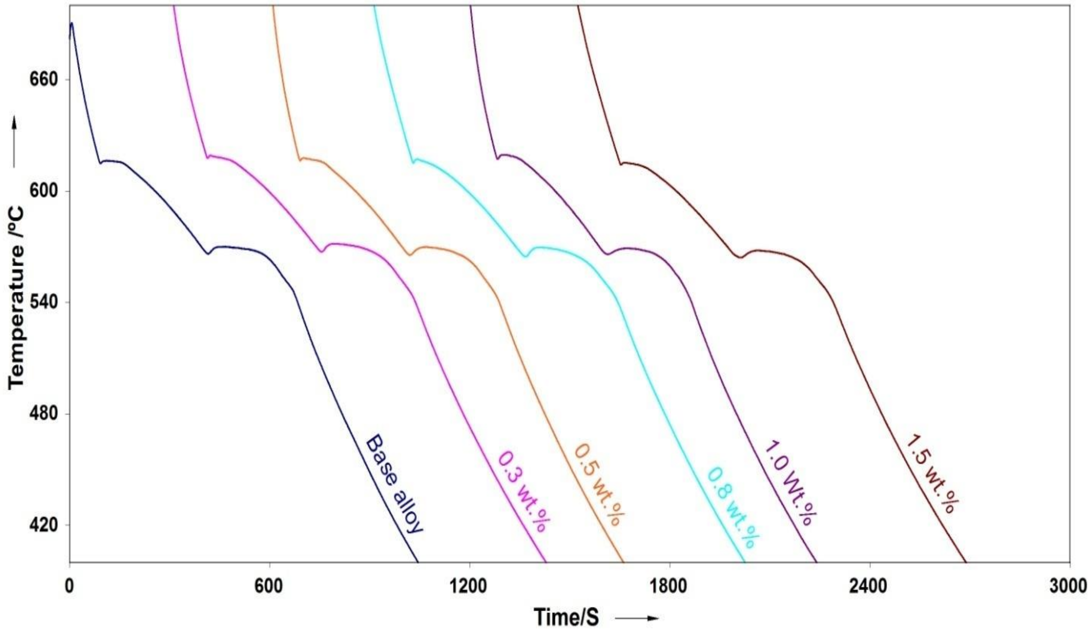

Fig. 1 - Cooling curve of base alloy and alloys treated with additions Ce and Er treated alloys

Table 1 - Cooling curve parameters of Al-phase for the base alloy with different concentrations of Ce and Er containing alloy identified during solidification by thermal analysis

Variables	**Parameters**					
	Growth		**Minimum**		**Nucleation**	
Wt.%	TGAl-Si/°C	t/s	TMAl-Si/°C	t/s	TNAl-Si/°C	t/s
0 wt.% Ce, Er	615.4	95.2	615.1	90.9	616.7	87.4
0.3 wt.% Ce, Er	618.3	118.6	617.7	114.4	619.6	111.2
0.5 wt.% Ce, Er	617.1	101.0	616.6	97.0	619.2	92.2
0.8 wt.% Ce, Er	617.2	101.0	616.7	96.1	616.5	92.3
1.0 wt.% Ce, Er	618.0	91.4	617.4	88.1	619.2	83.1
1.5 wt.% Ce, Er	614.7	162.8	614.3	157.8	615.5	154.7

It can be seen from Figure 2 that the addition of Ce, Er decreased the hypoeutectic growth temperature $T_G{}^{Al\text{-}Si}$. When the Ce, Er level was increased from 0.3 wt.% to 0.5 wt.%, the $T_G{}^{Al\text{-}Si}$ is not affected. However, when increasing the weight percent of Ce, Er was increased from 0.5 wt.% to 0.8 wt.%, the $T_G{}^{Al\text{-}Si}$ decreased continuously from 617.1 °C to 617.2 °C, but when 1.5 wt.% additive, a sharply drop of $T_G{}^{Al\text{-}Si}$ to 614.7 °C was observed. The decreasing of $T_G{}^{Al\text{-}Si}$ has a significant effect on the silicon morphology of Al-7Si-Mg alloys with the additives Ce, Er, and cooling as reported in [14]. As shown in Figure 2, little change of nucleation temperature T_N was observed with 0.1 wt.% Ce, Er the highest value compared with others, but it decreased 0.3 wt.% to 0.5 wt.% the $T_N{}^{Al\text{-}Si}$ decreased continuously from 619.2 °C to 616.5 °C, while the T_N Nucleation was increased from 0.3 wt.% to 0.5 wt.%. T_N was decreased from 0.8 wt.% to 1.5 wt.% Ce, Er a sharply drop of $T_N{}^{Al\text{-}Si}$ from 619.2 °C to 615.5 °C was observed. By 1.2 °C with 1.5 wt.% Ce, Er in comparison with base alloy measured at 616.7 °C in the base alloy. It can be seen that the addition of elements does affect not only the growth temperature but also the nucleation temperature. This is because additional atoms of the appropriate size can force twin nucleation at the solid-liquid interface. In this manner, the system requires a more considerable decrease in temperature as a driving force to start the nucleation step.

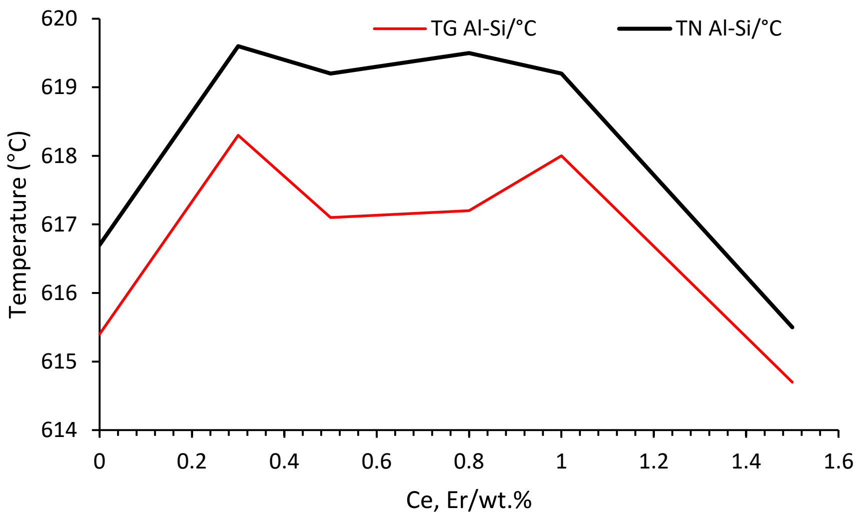

Fig. 2 - Changes of hypoeutectic growth temperature TG Al-Phase, and nucleation temperature TN Al-Phase with different concentration of Ce, Er

The depression in hypoeutectic growth temperature was used to evaluate the level of modification of the Si hypoeutectic phase after Ce, Er additions. However, it has been suggested that other parameters, such as nucleation and re-calescence characteristics of the hypoeutectic, should also be considered [10]. By observing the growth and minimum temperature, the recoalescence temperature ($\Delta TR = T_G^{Al\text{-}Si} - T_M^{Al\text{-}S}i$) can be computed as plotted in Figure 3. The alloys showed the lower re-calescence temperature of 0.3 °C, before Al-Si hypoeutectic growth temperature. However, the same re-calescence temperature was achieved with the amounts of 0.1 wt.% Ce, Er 0.8 wt.% Ce, Er, and 1.5 wt.% Ce, Er with little increment.

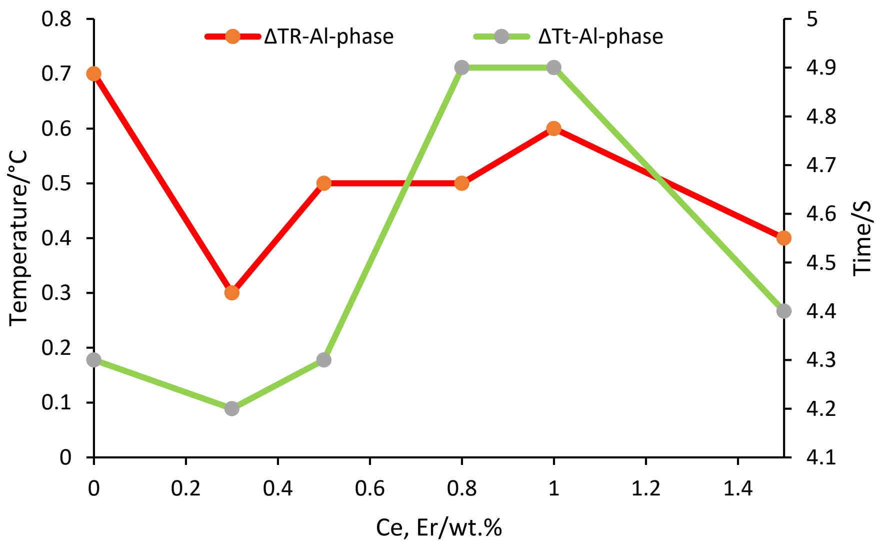

Fig. 3 - Effect of Ce, Er concentration on recoalescence temperature ΔTR Al-Phase and time ΔtR Al-Phase

Besides, the re-calescence time $\Delta T_R^{Al\text{-}Si}$ was increased continuously with the increase of Ce amount, as shown in Figure 3. For alloys with one wt.% Ce, it has a higher eutectic arrest time, which was measured at 33.4 s as compared to 22.3 s for the base alloy. The Ce additions show little changes on the re-calescence temperature, which can be estimated to be a modifier, as compared to the composite with Sr additive, which indicates 1.5 °C.

1.4 Al-Si phase

The characteristic parameters of the Al-Si phase have been determined by using the first and second derivatives and are reported in Table 2. The last stage of the solidification of Al-Si phase alloy is the formation of the Al- compound. As shown in Table 2, the Ce, Er additions was decreased the hypoeutectic growth from temperature $T_G^{Al\text{-}si}$ at 0.3 wt.% and 0.5 wt%, Ce, Er from 568.7 °C to 567.1 °C. Besides, when the Ce, Er addition was decreased at 1.0 wt% and 1.5 wt% was decreased respectively from 566.9 °C to 565.2 °C the temperature growth was 568.7 °C at 0.3 wt%. The $T_G^{AL\text{-}Si}$ increased continuously from the treated base alloy is increased with 0.3 wt.% Ce, Er additions. The temperature nucleation $T_N^{AL\text{-}Si}$ is increased at 0.5 wt.%, 0.8 wt.%, and 1.0 wt.%, and decreased at 0.3 wt.% and 0.5 wt.% Ce, Er from 598.2 °C to 566.7 °C. It can be seen in Figure 4, hypoeutectic growth temperature $T_G^{Al\text{-}Si}$ and (b) nucleation temperature $T_N^{Al\text{-}Si}$ with different concentrations of Ce, Er. In Figure 4, the effect of Ce, Er concentration on recalescence temperature $\Delta T_R^{Al\text{-}Si}$ and time $\Delta T_R^{Al\text{-}Si}$.

Table 2 - Cooling curve parameters of Al-Si phase for the base alloy with different concentrations of Ce identified during solidification by thermal analysis

Variables	Parameters					
	Growth		Minimum		Nucleation	
Wt.%	TGAl-Si/°C	t/s	TMAl-Si/°C	t/s	TNAl-Si/°C	t/s
0 wt.% Ce, Er	567.6	423.5	566.3	415.9	567.1	523.0
0.3 wt.% Ce, Er	568.7	466.4	567.3	457.9	598.2	450.6
0.5 wt.% Ce, Er	567.1	437.8	565.6	424.9	566.7	417.9
0.8 wt.% Ce, Er	566.7	435.8	565.6	426.2	567.1	415.9
1.0 wt.% Ce, Er	566.9	431.0	565.8	417.8	568.5	399.4
1.5 wt.% Ce, Er	565.2	528.7	564.3	420.4	567.0	492.0

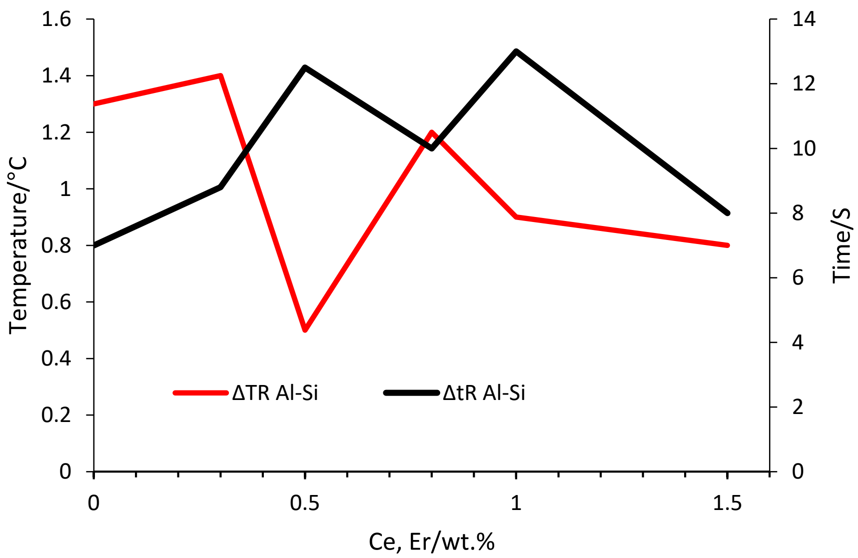

Fig. 4 - **Effect of Ce, Er concentration on recalescence temperature ΔTR Al-Si and time ΔtR Al-Si**

1.5 Mg-Si phase

The last stage in the solidification of Al-Si-Mg alloy is the formation of Al-Si-Mg compound. The characteristic parameters of Al-Mg phase are determined by using the first and second derivatives and are addressed in Table 3. The effect of Ce, Er addition on nucleation and growth temperature of the $T_N^{A\text{-}Mg}$ is plotted in Figure 8 and shows that $T_N^{Al\text{-}Mg}$ increased linearly by concentrations 0.5 wt.% Ce and 0.8 wt.% Ce, Er, which was measured at temperature 554 °C, 554.2 °C and 555.5 °C at 1.0 wt.% Ce, Er respectively and compared with that of base alloy 554.5 °C. The characteristic parameters of Al-Mg phase are determined by using the first and second derivatives and are presented in Table 3.

Table 3 - Cooling curve parameters of Al-Mg phase for the base alloy with different concentrations of Ce, Er identified during solidification by thermal analysis

Variables	Parameters					
	Growth		Minimum		Nucleation	
Wt.%	TG Al-Si/°C	t/s	TS Al-Si/°C	t/s	TN Al-Si/°C	t/s
0 wt.% Ce, Er	549.7	660.1	539.8	684.0	554.6	636.0
0.3 wt.% Ce, Er	550.0	706.6	538.7	742.5	555.2	684.5
0.5 wt.% Ce, Er	549.6	664.5	537.0	701.4	554.0	646.3
0.8 wt.% Ce, Er	549.4	665.3	538.5	698.4	554.2	645.5
1.0 wt.% Ce, Er	554.4	626.3	537.3	675.0	555.4	623.0
1.5 wt.% Ce, Er	548.9	765.3	539.1	820.3	552.9	746.9

As can be seen in Table 3, Ce, Er has a significant effect on $T_G^{Al\text{-}Mg}$ characteristic, whereby $T_G^{Al\text{-}Mg}$ increased with increasing of Ce, Er amount. As shown in Figure 5, the Ce additives were affected in the last phase of the solidification. In a similar trend, Figure 5 shows the temperature at the end of the solidification stage and it shows that the increase in the level of Ce also increased the end of the solidification stage of alloys.

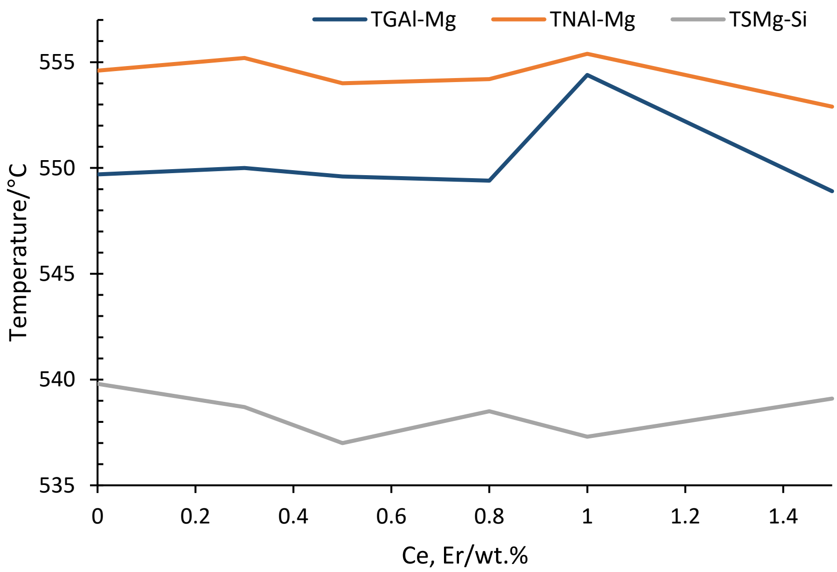

Fig. 5 - Variation of TGAl-Mg, TNAl-Mg for base alloy and different concentrations of Ce, Er addition and end of solidification temperature TSMg-Si of base alloy and different Ce levels in the alloy

Based on the results of Al-Si and Al-Mg phases that are observed in Tables and, the solidification range for the formation of Al-Si phase can be determined by ($\Delta T^{Al\ Si} = TN^{Al\text{-}Si} - TN^{Al\text{-}Mg}$) as plotted in Figure. There are no significant changes observed with the increase of Ce, Er levels from 0.1 wt.% to 0.3 wt.% on the formation of Al-Si hypoeutectic. A decreasing trend can be observed when Ce, Er was increased from 0.5 wt.% to 1.0 wt.%. Thus, the effect of Ce, Er additives can be found during each hypoeutectic phase formation on Al-Si and Al-Mg; that is when the Ce, Er amount is increased from 0.5 wt.% to 1.0 wt.%. When the effects of element addition are investigated in terms of the depression of hypoeutectic growth temperature and that shows significant differences between the results of Ce and Er as observed. The addition of Ce, Er modifier produced more changes in the hypoeutectic growth depression ΔTG and re-calescence, as compared to those noted when Ce, Er composition are added.

1.6 Microstructure analysis

For microstructural examination purposes, samples were prepared from the thermal analysis casting and examined using various metallographic techniques such as optical microscopy, porosity measurement, and phase identification. However, the microstructure developed during the solidification is dependent not only on the nucleation potential and modification potential of the melt but also on the thermal gradient imposed during solidification. Thus, the characteristic cooling curve parameters are correlated with the proper state of nucleation and modification in the melt required to produce the desired microstructure in a specific casting section size [16]. The microstructures of Al-7Si-0.3Mg alloy with 0 wt.%, 0.3 wt.%, 0.5 wt.%, 0.8 wt.%, 1.0 wt.% and 1.5 wt.% Ce, Er contents, respectively. It is seen that the microstructure consists of a large number of platelets, as shown in Figure 6.

Moreover, the coarse acicular and plate-like hypoeutectic Si structure transformed into a branched structure with a decrease in silica size at 0.3 wt.% Ce, Er. Alloy containing 0.8 wt.% Ce shows a very irregular, longitudinal sharp-edged structures and then transform to a more practical, smaller refiner silica with high level; 1.0 wt.% Ce. Image analyses of base alloys with different concentrations of Ce addition, as shown in figure 7**.**

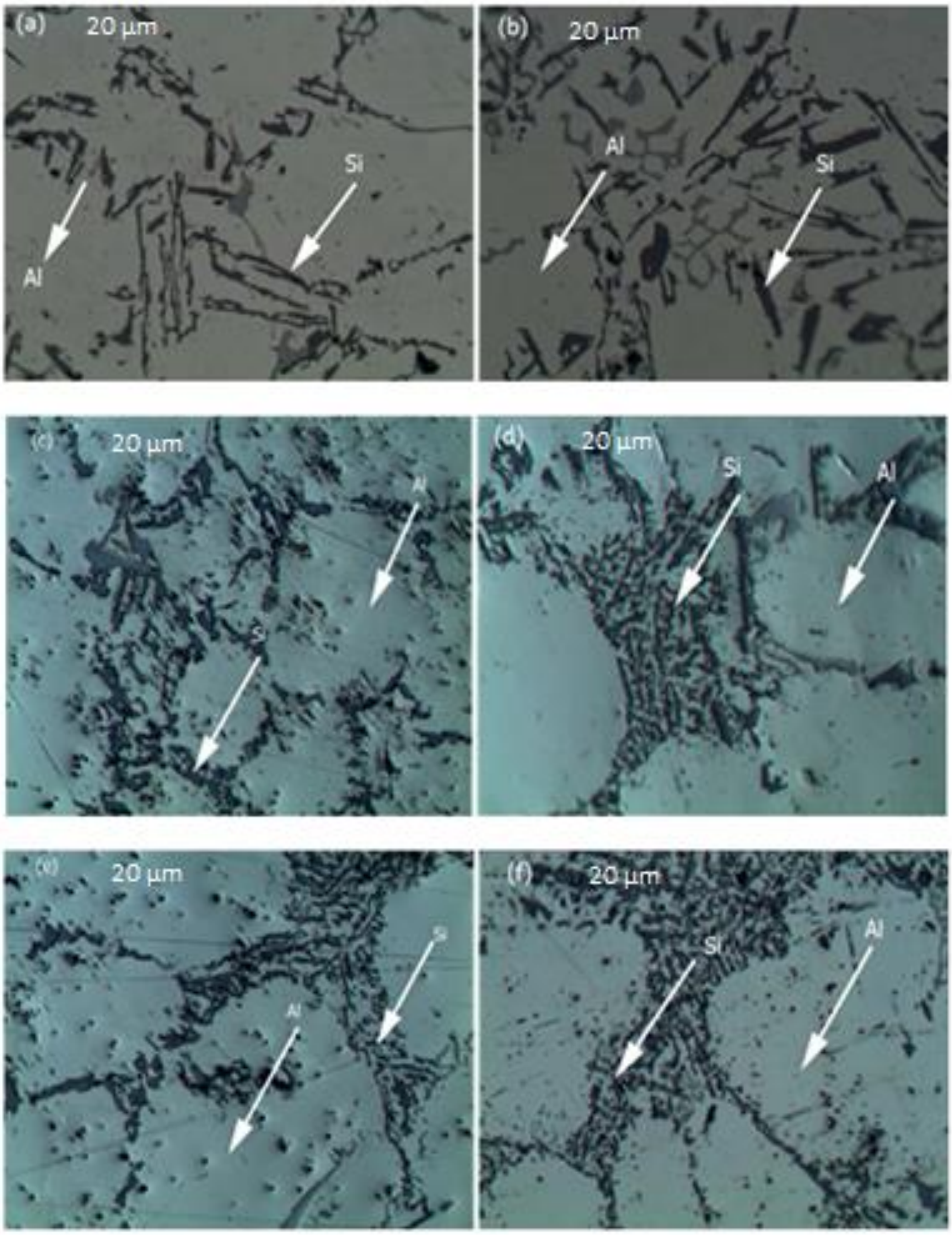

Fig. 6 - Optical microstructure image of (a) Base alloy; (b) 0.3 wt.% Ce, Er; (c) 0.5 wt.% Ce, Er (d); 0.8 wt.% Ce, Er; (e) 1.0 wt.% Ce, Er; (f) 1.5 wt.% Ce, Er

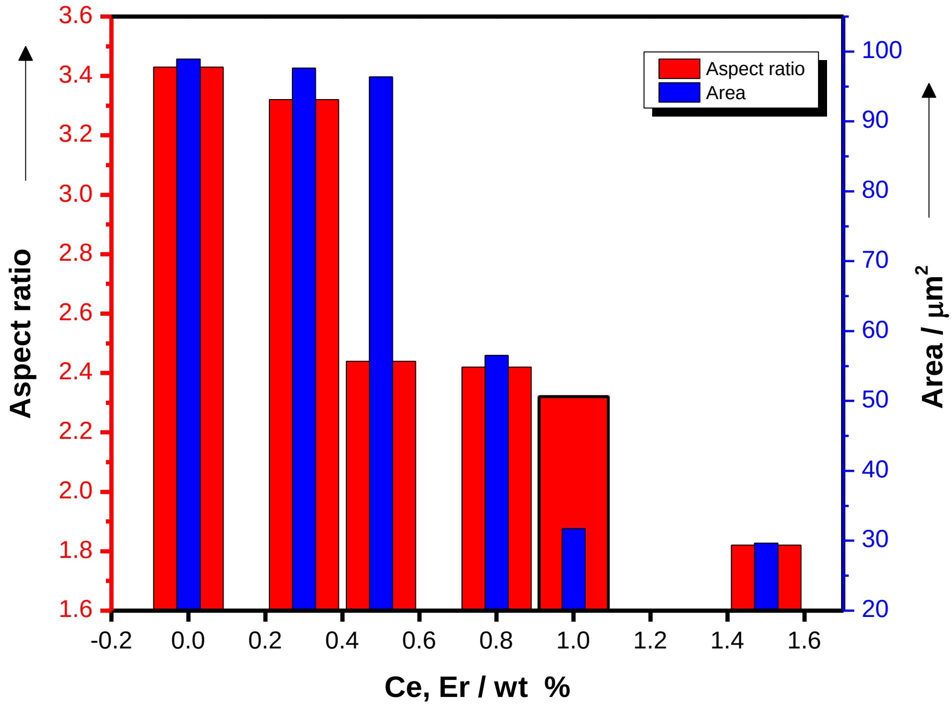

Fig. 7 - Image analyses of base alloys with different concentrations of Ce addition

SEM/EDS micro-analysis on the scanning electron microscope the effect of the Ce, Er addition on the SDAS is plotted in Figure 8, which was used to identify the chemical intermetallic composition of the phases present in the alloy. It is well known that the Ce, Er have limited solid solubility in aluminium under equilibrium condition, and Ce, Er are energetic, active elements, which can efficiently react with Al or Si atom [5]. The microstructure of all the standard microstructure elements characteristics for this type of the alloy was found, i.e., primary crystals of α Al, eutectics (α Al $+_{\beta}$Si) and (αAl+Mg2Si), Al-Fe-Si and Al-Mg phase. Table 4 presents the chemical compositions of Ce; Er formed intermetallic compound as a combination of Al, Ce, Er and Si which solidified in rounded polyhedral shape. Also, Table 4 shows the Ce; Er had the second position in chemical empirical which means the compounds are abundant in Ce and Er. Furthermore, the Ce, Er elements have a high tendency to forming a mixture, and this is because there is a big difference in atomic radius, where for Ce is 5.27 and Er 3.42 at Al 39.72 and 19.13 respectively. For this reason, Ce in these alloys formed intermetallic compounds [18].

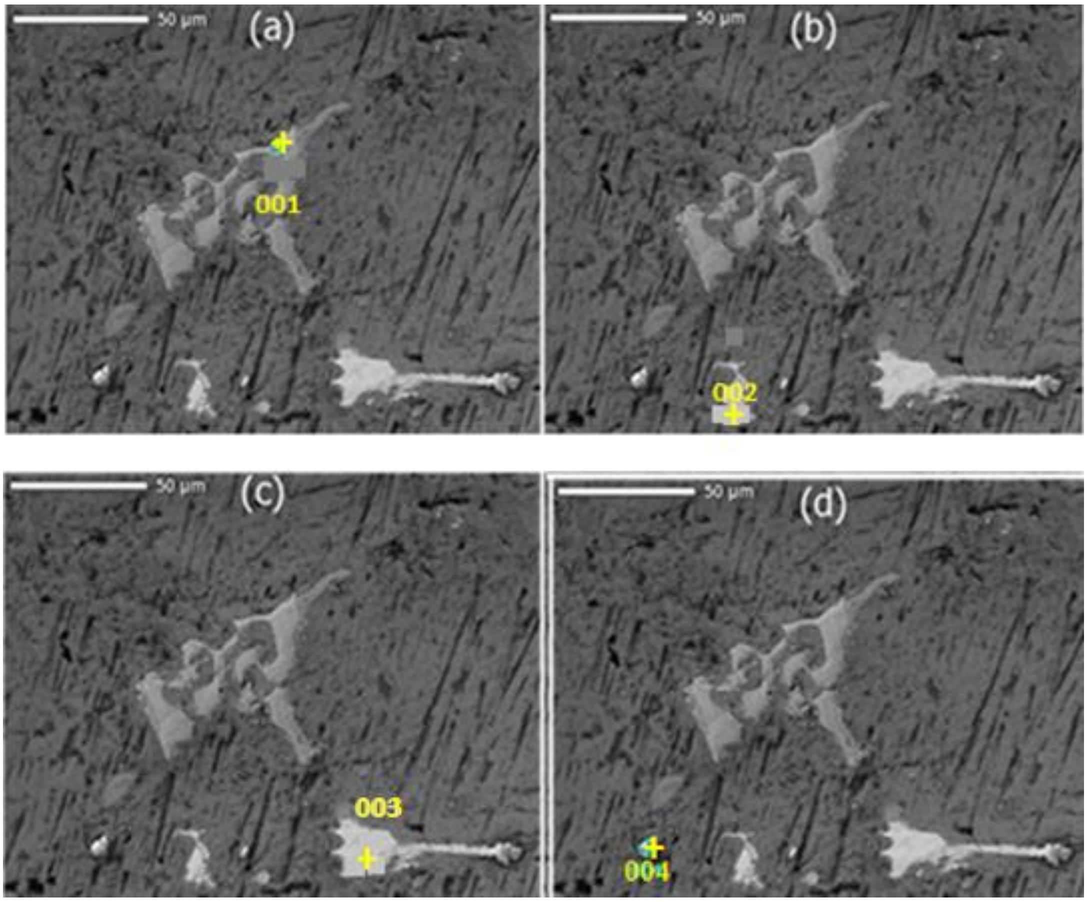

Fig. 8 - SEM/EDS micrograph of the specimen without and with 1.5 wt.% Ce, Er (a) Al-Si-Fe-Er; (b) Al-Si-Ce-Er; (c) Al-Si-Ce-Er; (d) Al-Si

Table 4 - Chemical composition of Ce, Er- intermetallic phases

Intermetallic phases	Chemical structure, wt.%				
	AL	Si	Fe	Ce	Er
Al-Si-Fe-Er	74.78	11.54	9.83	-	3.35
Al-Si-Ce-Er	39.72	37.57	-	15.97	6.74
Al-Si-Ce-Er	19.13	40.0	-	10.70	10.16
Al-Si	1.57	98.43	-	-	-

The Ce, Er compound combined with Al and Si was found to be as long interfacing with Al-Si hypoeutectic, where Ce, Er compounds are found along with the interface of hypoeutectic Si-Al or at the edge of the primary Si crystals. In addition, it is well known that Ce and Er are types of surface-active agents. The result of SEM/EDS shows that the reaction of additions Ce, Er formed compounds with alloy elements such as Al, Si, Mg and forming compounds such as Al-Si-Fe-Er, Al-Si-Ce-Er, Al-Si-Ce-Er, and Al-Si, which shows the variation in chemical composition. The benefit of cooling curve thermal analysis is to determine the particular points of metallurgical reactions during solidification. The results of the cooling curve and microstructure can clearly show the effect of Ce, Er additive on Al-7Si-0.3Mg casting alloy. The decrease in growth and nucleation temperature was continuous with the increase of Ce, Er amount, which led to the reduction of the refiner of the silica structure.

1.7 Conclusions

Based on the results obtained in this research, the characteristic parameters of the Al-Si phase have been determined. The cooling curves thermal analysis results show that the growth $TG^{Al\text{-}Si}$ and nucleation $T_N^{Al\text{-}Si}$ temperatures increased temperatures 566.9 °C and 568.5 °C, respectively as the amount Ce, Er increased to 1.0 wt.%. The last stage of solidification of Al-Si-Mg alloy is the formation of Al-Si-Mg Compound. The results show that the growth $T_G^{Al\text{-}Mg}$ and nucleation TN $^{Al\text{-}Mg}$ temperatures increased temperatures 549.4 °C and 554.2°C, respectively as the amount Ce, Er increased to 0.8 wt. %.Based on microstructure observations, the Si structure of Al-Si-Mg changed from flake–plate-like to very irregular, longitudinal sharp-edged structures and became a more practical, smaller refiner silica with 1.0 wt.% Ce, Er, while the size of Si particles reduced compared with base alloy. A high amount of Ce, Er (1.5%) addition reduces the size of the platelet Si-intermetallic to excellent form. Maximum improvement in impact strength has been achieved by 1.5% Ce, Er addition to AI-7Si alloy.

Acknowledgement

The authors wish to thank University Technology Malaysia and Ministry of Higher Education, Malaysia, for their assistance throughout conducting this research. Special appreciation to the Research Management Centre of UTM for the financial support through the RUG funding Q. J130000.3551.07G23.

References

[1] Ahmad, R., Talib, N., & Asmael, M. (2013). Effect of pouring temperature on microstructure properties of Al-Si LM6 Alloy sand casting. Paper presented at the Applied Mechanics and Materials.
[2] Backerud, L., Chai, G., & Tamminen, J. (1990). Solidification characteristics of aluminium alloys. Vol. 2. Foundry alloys. American Foundrymen's Society, Inc., 1990, 266.
[3] Borgeson, W. C., Henjum, H. E., & Whitnah, G. R. (1964). Balloon construction. In: Google Patents.
[4] Burns, T. (2017). The Foseco foundryman's handbook: facts, figures and formulae: Elsevier.
[5] Farahany, S., Ourdjini, A., Bakar, T. A. A., & Idris, M. H. (2014). A new approach to assess the effects of Sr and Bi interaction in ADC12 Al-Si die casting alloy. Thermochimica Acta, 575, 179-187.
[6] Farahany, S., Ourdjini, A., Idrsi, M., & Shabestari, S. (2013). Evaluation of the effect of Bi, Sb, Sr and cooling condition on eutectic phases in an Al-Si–Cu alloy (ADC12) by in situ thermal analysis. Thermochimica Acta, 559, 59-68.
[7] Gschneidner, K., & Calderwood, F. (1988). The Al− Ce (Aluminum-Cerium) system. Bulletin of Alloy Phase Diagrams, 9(6), 669-672.
[8] Jayakumar, A., & Rangaraj, M. (2014). Property analysis of aluminium (LM-25) metal matrix composite. International Journal of Emerging Technology and Advanced Engineering, 4(2), 495-501.
[9] Kaufman, J. G., & Rooy, E. L. (2004). Aluminium alloy castings: properties, processes, and applications: Asm International.
[10] Knuutinen, A., Nogita, K., McDonald, S., & Dahle, A. (2001). Modification of Al-Si alloys with Ba, Ca, Y and Yb. Journal of Light Metals, 1(4), 229-240.
[11] Kuppuswamy, R. (2011). Metallographic etching of aluminium and its alloys for the restoration of obliterated marks in forensic science practice and investigations. In Aluminium Alloys, Theory and Applications: InTech.
[12] Machovec, C., Byczynski, G., Zindel, J., & Godlewski, L. (2000). Effect of Bi-Sr interactions on Si morphology in a 319-type aluminium alloy. Paper presented at the Transactions of the American Foundry Society and the One Hundred Fourth Annual Castings Congress.
[13] Nayak, S., & KVNB, A. K. (2011). Synthesis of Al-Si Alloys and study of their Mechanical properties.
[14] Nordin, N. A., Farahany, S., Ourdjini, A., Bakar, T. A. A., & Hamzah, E. (2013). Refinement of Mg2Si reinforcement in a commercial Al–20% Mg2Si in-situ composite with bismuth, antimony and strontium. Materials Characterization, 86, 97-107.
[15] Shapiro, M. F., Hatch, R. L., & Greenfield, S. (1984). Cost containment and labour-intensive tests: the case of the leukocyte differential count. JAMA, 252(2), 231-234.
[16] Speyer, R. (1993). Thermal analysis of materials: CRC press.
[17] Taylor, J. A. (2012). Iron-containing intermetallic phases in Al-Si based casting alloys. Procedia Materials Science, 1, 19-33.
[18] Vončina, M., Kores, S., Mrvar, P., & Medved, J. (2011). Effect of Ce on solidification and mechanical properties of A360 alloy. Journal of Alloys and Compounds, 509(27), 7349-7355.